

Time-resolved diffraction profiles and structural dynamics of Ni film under short laser pulse irradiation

Zhibin Lin and Leonid V. Zhigilei*

University of Virginia, Department of Materials Science and Engineering
116 Engineer's Way, Charlottesville, VA 22904-4745

* E-mail: lz2n@virginia.edu

Abstract. The evolution of the diffraction profiles during the fast thermoelastic deformation and structural transformations induced in a thin Ni film by short pulse laser irradiation is investigated in molecular dynamics simulations. Fast disappearance of the diffraction peaks characteristic for the initial crystal structure is related to the homogeneous nucleation and growth of liquid regions inside the overheated crystal. Transient thermoelastic deformation of the film prior to melting is reflected in shifts and splittings of the diffraction peaks, providing an opportunity for experimental probing of the ultrafast deformations.

1. Introduction

Short (pico- and femtosecond) pulse laser irradiation has the ability to bring material into a highly non-equilibrium state and opens up a unique opportunity to study the transient atomic dynamics under extreme conditions that can hardly be achieved by any other means. Recent advances in time-resolved x-ray and electron diffraction pump-probe techniques provide new means to explore the ultrafast phase transformations, e.g. [1,2]. Atomistic simulations can serve as a bridge between the experimental observations and atomic-level structural changes in the irradiated material [3] and help in interpretation of experimental data. In this paper we report the results of molecular dynamic (MD) simulations of short pulse laser interactions with thin free-standing Ni films. The diffraction profiles are calculated from the transient atomic configurations obtained in the simulations. The evolution of the characteristic features of the diffraction profiles is related to the fast thermoelastic deformation and atomic-level dynamics of structural transformations revealed in the simulations.

2. Computational model: MD simulation setup and calculation of diffraction profiles

Simulations presented in this paper are performed with a hybrid atomistic-continuum model combining classical MD method for simulation of nonequilibrium processes of lattice superheating and fast phase transformations with a continuum description of the laser excitation and subsequent relaxation of the conduction band electrons [3]. Laser-induced atomic dynamics is investigated for a free-standing 21 nm Ni film irradiated with a 200 fs laser pulse at a range of absorbed fluences, from 10 mJ/cm² to 30 mJ/cm². The initial MD system is an FCC crystal composed of 864,000 Ni atoms with dimensions of 21.19×21.19×21.19 nm and periodic boundary conditions imposed in the directions parallel to two (001) free surfaces. The initial system is equilibrated at 300 K and zero pressure. The embedded-atom method in the functional form and parameterization suggested in Ref. [4] is used to describe the interatomic interaction in the MD part of the model. The properties of the EAM Ni material and the parameters used in the continuum part of the model are given in Ref. [3].

In order to calculate diffraction profiles from atomic configurations generated in MD simulations, we consider elastic scattering of a beam of X-ray photons or electrons on a sample consisting of N atoms. Following the well-known Debye scattering equation [5], one can substitute the summation over atomic pairs by the pair density function $\rho(r)$ and define the structure function $S(Q)$ [6] as

$$S(Q) = 1 + \int_0^{\infty} 4\pi r^2 \rho(r) \frac{\sin(Qr)}{Qr} dr, \quad (1)$$

where Q is the magnitude of the scattering vector. The pair density function $\rho(r)$ can be calculated from the atomic coordinates obtained in the simulations,

$$\rho(r) = \frac{1}{4\pi N r^2} \sum_{j=1}^N \sum_{i=1}^N \delta(r - r_{ij}), \quad (2)$$

where r_{ij} is the distance between atoms i and j and δ is the Dirac delta function. In order to reduce spurious ripples from the termination of the pair density function at a finite distance R_{max} , a damping function $W(r) = \sin(\pi r / R_{max}) / (\pi r / R_{max})$ [7] is used in Equation (1), resulting in:

$$S(Q) = 1 + \int_0^{R_{max}} 4\pi r^2 \rho(r) \frac{\sin(Qr)}{Qr} W(r) dr, \quad (3)$$

where R_{max} is chosen to be half of the size of the simulation box. More detailed discussion of the effect of the finite size of the system and the termination ripples is given in Ref. [7].

3. Results and discussions

Figure 1 shows the time evolution of the laser melting process predicted in the simulations of a 21 nm Ni film irradiated with a 200 fs laser pulse at absorbed fluences ranging from 15 mJ/cm² to 30 mJ/cm². Two distinct regimes can be easily identified: a high-fluence regime when the entire film melts within a few picoseconds, and a low-fluence regime when the melting starting time increases sharply with decreasing fluence and the melting process slows down significantly. It is found that in the high-fluence regime, above 20 mJ/cm², homogeneous nucleation of liquid regions is observed throughout the film, whereas in the low-fluence regime, at and below 16 mJ/cm² melting takes place only by propagation of melting fronts from free surfaces. The laser energy absorbed by the film in the low-fluence regime, at and below 16 mJ/cm², is not sufficient for the complete melting the system and a partially melted film equilibrated at the melting temperature is observed at the end of the simulation.

In order to investigate the ultrafast structural transformation during the melting process in the high-fluence regime, we choose the result from the simulation performed at an absorbed fluence of 20 mJ/cm². Figure 2 shows the results from the calculation of the structure functions at 0 ps, 12 ps, 15 ps and 20 ps after the laser pulse. It can be seen that before the laser excitation, the peaks of the structure

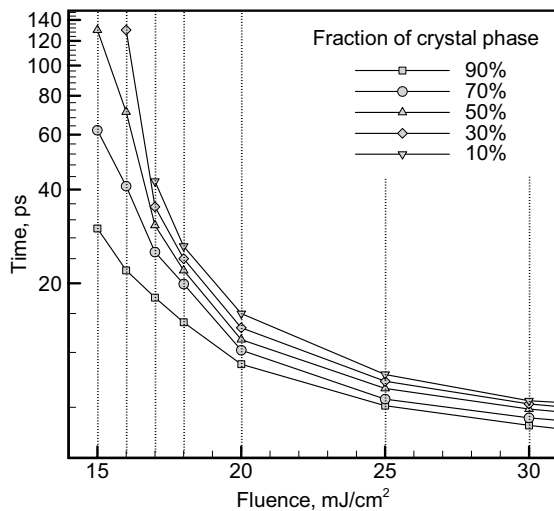


Figure 1. Semi-log plots showing the timescales of the melting process in a 21 nm Ni film irradiated with a 200 fs laser pulse at different absorbed fluences. Each curve corresponds to a certain fraction of the remaining crystal phase as a function of the absorbed fluence. For example, the curve with squares corresponds to the time after laser excitation when 90% of the atoms in the film belong to the crystal phase. The fraction of the crystal phase is determined by the number of atoms with local crystalline environment, as predicted by the local order parameter [3].

function can be easily identified and associated with the Miller indices for FCC structure, Figure 2(a). By the time of 12 ps, however, the structure function has changed significantly, Figure 2(b). Although at this time about 77% of atoms still maintain their local crystalline surroundings, the height of all the peaks have been largely reduced. This reduction can be only partially attributed to the increasing thermal vibrations of the atoms (Debye-Waller effect) [5,7], with an additional contribution coming from the onset of the structural changes (melting). In fact, by the time of 12 ps the energy transfer from the hot electrons to the lattice has lead to the lattice overheating by $\sim 14\%$ above the equilibrium melting temperature of the model Ni material. This overheating, combined with the uniaxial thermoelastic deformation of the film [8], is sufficient to induce the homogeneous nucleation of a large number of liquid regions inside the film, effectively destabilizing the lattice and reducing the long-range order throughout the film, as is apparent from the snapshot shown in Figure 2(b). The homogeneous nucleation and growth of the liquid regions leads to a fast melting of the entire film within several picoseconds. Although at 15 ps several crystalline regions can be still observed in the snapshot given in Figure 2(c), the structure function is close to the one at 20 ps, when the loss of crystalline order throughout the film is apparent.

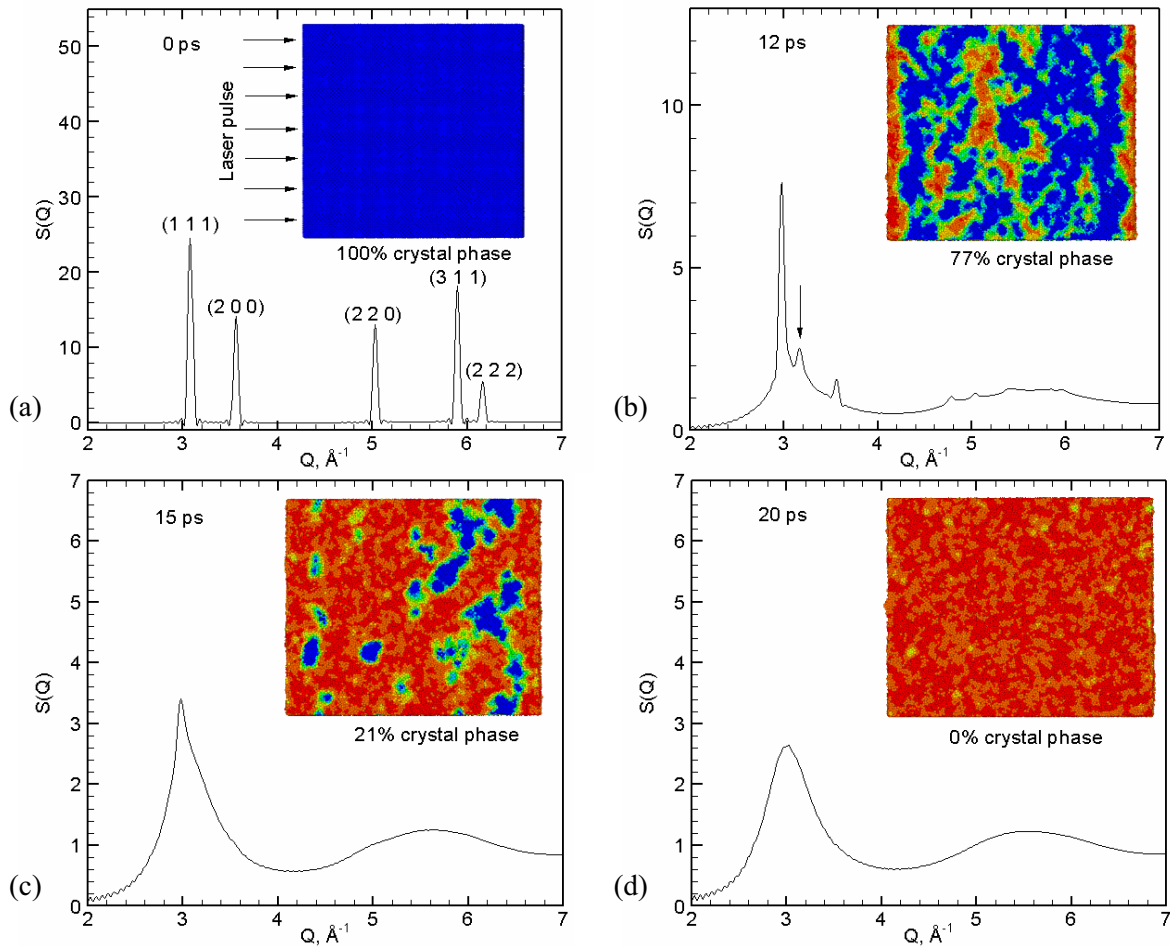


Figure 2. Structure functions calculated for atomic configurations obtained in a simulation of 21 nm Ni film irradiated with a 200 fs laser pulse at an absorbed fluence of 200 J/m^2 at (a) $t = 0 \text{ ps}$, (b) $t = 12 \text{ ps}$, (c) $t = 15 \text{ ps}$, (d) $t = 20 \text{ ps}$. Insets show the corresponding snapshots of the atomic configurations, with the direction of the laser pulse shown in (a). Atoms are colored according to the local order parameter (blue atoms have local crystalline surroundings; red atoms belong to the liquid phase). The arrow in (b) points to the (002) peak that separates from the (200)/(020) peaks in the process of uniaxial expansion of the film in the direction normal to the free surfaces.

An interesting observation from the analysis of the evolution of the structure function is the appearance of new peaks, such as the one indicated by the arrow in Figure 2(b). This peak first appears at 4 ps by splitting from the (200) peak and continues shifting to the left at later times. We find that the splitting of the peaks is a direct consequence of the uniaxial thermoelastic deformation of the film in response to the laser heating. Thermoelastic stresses generated by the fast heating of the lattice can only relax by the film expansion in the direction normal to the free surfaces of the film. The uniaxial deformation of the original FCC lattice along the (001) direction changes the space group symmetry of the lattice in a way that the cubic lattice transforms into the tetragonal one. The new peak could be identified by the Miller indices as (002) that is distinct from the (200)/(020) peak in the Face Centered Tetragonal (FCT) lattice.

To further illustrate the effect of thermoelastic deformation on the structure function we use the results from a simulation performed at an absorbed fluence of 10 mJ/cm^2 , at which no melting is observed. It can be seen that right after laser excitation, both (111) and (002) peaks shift to the left due to the uniaxial expansion of the film and reach the leftmost positions by the time of 8 ps. From the position of (002) peak, one can estimate the lattice deformation along (001) direction at 8 ps to be $\sim 4.5\%$, which is consistent with the direct measurement of the thickness of the film in the atomic-level snapshot. As the relaxation of the initial compressive stresses leads to the uniaxial expansion of the film, tensile stresses are generated in the middle part of the film, pulling the film back and decreasing the deformation of the lattice. As a result, both (111) and (002) peaks shift back to the right from 8 ps to 13 ps. The process repeats itself at later times as the elastic oscillation of the film continue with amplitude gradually decreasing due to the dissipation of the pressure wave trapped inside the film. Similar shifts/oscillations are observed for other peaks of the structure function with the maximum value of the peak displacement defined by the orientation of the corresponding lattice planes with respect to the direction of the film expansion.

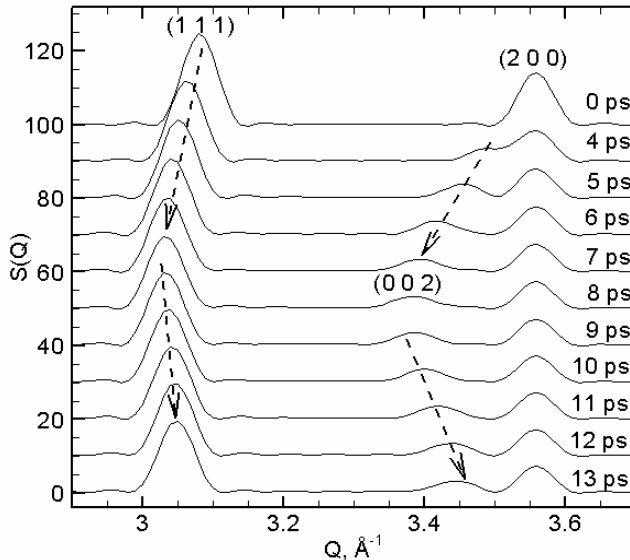


Figure 3. Structure functions calculated for 21 nm Ni film irradiated with a 200 fs laser pulse at an absorbed fluence of 10 mJ/cm^2 . Curves are shifted with respect to each other in order to better illustrate the shift of the diffraction peaks, indicated by the arrows. Diffraction peaks are identified by the Miller indices as shown in the brackets.

Note that the structure functions plotted in Figures 2 and 3 include the information on all the lattice plane systems present in the crystal. In polycrystalline samples different orientations of crystallographic planes will be affected in a different way by the uniaxial expansion of the film and the structure function would exhibit broadening of the peaks instead of the splitting. In experiments performed with a fixed angle of incidence of the probe beam to the target surface, only the lattice planes that have the correct Bragg angle with the probe beam contribute to the measured diffraction spectrum. Splitting of the peaks can only be observed experimentally if probing is done at different incidence angles, so that different orientations of the same system of lattice planes with respect to the direction of the thermoelastic lattice expansion is probed. Nevertheless, for a given direction of the

probe beam, analysis of the peak shifts in time-resolved X-ray or electron diffraction experiments can provide valuable information on the characteristic time-scale of lattice heating and thermoelastic deformation as well as on the role of the uniaxial deformation in laser-induced phase transformations. Indeed, the evolution of the lattice deformation in a Au(111) single crystal following a short pulse laser heating has been measured with ~ 10 ps temporal resolution in X-ray diffraction experiments and related to the kinetics of the lattice temperature evolution in the surface region of the irradiated crystal [9]. Periodic oscillations of the diffraction peak positions have been recently probed with ~ 0.5 ps resolution in electron diffraction experiments performed for a free standing polycrystalline Al film irradiated with a femtosecond laser pulse [10,11]. The oscillations of the diffraction peak positions have the same origin as the ones shown in Figure 3, albeit the values of the maximum shifts are much smaller since the planes having a small Bragg angle are probed by an electron beam normal to the surface of the film.

4. Conclusions

The atomic-level dynamics of structural transformations in a thin Ni film irradiated by a short laser pulse are investigated in MD simulations and related to the evolution of the diffraction profiles. Fast disappearance of the diffraction peaks characteristic for the initial crystal structure is observed in the simulations performed at high laser fluences and is related to the homogeneous melting of the film. The melting process takes only several picoseconds, in agreement with the results of recent time-resolved electron diffraction experiments [1]. Shifts and splittings of the diffraction peaks are found to reflect the transient uniaxial thermoelastic deformation of the film prior to melting, providing an opportunity for probing the ultrafast deformations in experiments [10,11].

Acknowledgments

Financial support of this work is provided by the NSF through award CTS-0348503 and by the ONR through a sub-contract from the Electro-Optics Center, Penn State University.

5. References

- [1] Siwick B J, Dwyer J R, Jordan R E and Miller R J D 2003 *Science* **302**, 1382
- [2] Lindenberg A M et al. 2005 *Science* **308**, 392
- [3] Ivanov D S and L V Zhigilei 2003 *Phys. Rev. B* **68**, 064114
- [4] Zhou X W et al 2001 *Acta Mater.* **49**, 4005
- [5] Warren B E 1969 *X-Ray Diffraction* (Reading: Addison-Wesley)
- [6] Egami T and Billinge S J L 2003 *Underneath the Bragg Peaks: Structural analysis of complex materials* (Amsterdam: Elsevier)
- [7] Lin Z and Zhigilei L V 2006 *Phys. Rev. B* **73**, 184113
- [8] Ivanov D S and Zhigilei L V 2003 *Phys. Rev. Lett.* **91**, 105701
- [9] Chen P, Tomov I V and Rentzepis P M 1996 *J. Chem. Phys.* **104**, 10001
- [10] Park H, Nie S, Wang X, Clinite R and Cao J 2005 *J. Phys. Chem. B* **109**, 13854
- [11] Park H, Wang X, Nie S, Clinite R and Cao J 2005 *Solid State Commun.* **136**, 559